An efficiency paradox of uberization

Kenan Zhang,[1†] Hongyu Chen,[1†] Song Yao,[2] Linli Xu,[2] Jiaoju Ge,[3]
Xiaobo Liu,[4] Yu (Marco) Nie[1*]

[1]Department of Civil and Environmental Engineering, Northwestern University, IL 60208, USA
[2]Carlson School of Management, University of Minnesota, MN 55455, USA
[3]Harbin Institute of Technology Shenzhen Graduate School, Shenzhen, China
[4]School of Transportation and Logistics, Southwest Jiaotong University, Chengdu, China
[†]These authors contributed equally to this work.
[*]Correspondence to: y-nie@northwestern.edu

Efficient peer-to-peer matching both enables and undermines the success of uberization in transportation.

Uberization promises to transform society based on an intuitive proposition: Advanced peer-to-peer matching guarantees greater overall efficiency. Here we show a paradox challenging this proposition in uberized ride-hail service, known as *e-hail*. By analyzing hundreds of local markets in Shenzhen, China, we discover e-hail is outperformed—in terms of wait time and trip production—by taxis hailed off street in areas with high densities of passengers and drivers. This paradox arises because a quicker match does not always expedite and enhance a service. On the contrary, it can induce competition that undermines the network effect, making a passenger less likely to benefit from more drivers, and vice versa, in e-hail than in taxi service. Consequently, simply attracting more users may not improve e-hail's efficiency, because its competitive edge

diminishes with scale. The finding implies uberization has a limited impact on efficiency and is *unlikely* to create a "winner-take-all" in transportation.

Introduction

Thanks to the advance of mobile technology, activities that once depended on physical interactions can now be accomplished at one's fingertips. This innovation enables consumers and providers of a service to match on a digital platform in real-time and enjoy a reduced transaction cost (*1, 2*). The launch of Uber set in motion the rapid adoption of this new business model—known as uberization (*3*)—in many aspects of our daily life (*4, 5*). Users are attracted to a uberized service platform by the prospect of greater convenience and efficiency, and their accumulation on the platform triggers a *cross-side network effect*; that is, a larger number of users on one side of the market makes the service more appealing to users on the other side (*6–8*). In turn, this effect creates a positive feedback loop that keeps growing the platform and projects a prospect of "winner-take-all." Blessed with this *virtuous cycle*, uberization is expected to transform and even dominate the way many services are provided and consumed (*2*), which would have a far-reaching societal impact.

Although uberization continues to gain momentum around the world, whether and when it will deliver on the above promises remains unclear. Many uberized service platforms, Uber itself included, have yet to turn a profit (*9*). Also, outgrowing others does not seem to ensure dominance, as big platforms such as Airbnb and Uber have not been able to drive their much smaller competitors out of the market (*10*). Here we show the seeming growing pains of a new economic paradigm may have a more fundamental cause: The virtuous cycle of uberization is checked by an *efficiency paradox*.

We choose to demonstrate the efficiency paradox in the ride-hail industry (*11–15*), where uberization originated. Thanks to its advanced matching technology, uberized ride-hail service,

known as the *e-hail* service, has been praised for less wait time and higher productivity, compared to its antiquated competitor: *taxis* hailed off street (*16,17*). Yet, few studies have validated this claim with empirical evidence. Hence, our inquiries start from comparing the operational performance of e-hail and taxis. The data used in the analysis were collected in Shenzhen, a megacity in China with more than 13 million residents and a dense urban core surrounded by an expansive metropolitan area. In 2015, roughly 300,000 daily taxi trips were served by a fleet of 15,000 taxis, on par with the activities seen in New York City (*18*). Several e-hail services have been launched in Shenzhen since 2014, and the one analyzed in this report serves a number of daily trips comparable to that of taxis.

Results

The data were collected for a full week in 2016. For each day of the week, we first aggregate the data for two three-hour periods and 277 local markets located in six municipal districts of the city; see [S1.2] in *Supplementary Materials* and Fig. S1. Fig. 1 examines average wait time ($\bar{w}$), vacant vehicle density (Λ), and pickup rate (m) at the district level. Λ consists of both matched (Λ_1) and unmatched (Λ_0) vacant vehicles. The former refers to those en route to pick up passengers, and the latter refers to those waiting to be matched. Hence, for e-hail, $\Lambda = \Lambda_0 + \Lambda_1$, and for taxis, $\Lambda = \Lambda_0$. The results show e-hail produces more pickups than taxis in districts with a relatively low density of passengers and drivers (e.g., suburbs S-1 and S-2), but falls behind in high-density downtown districts (i.e., D-1 and D-2). Taxi wait time varies across the districts much more than e-hail, and is significantly lower in downtown than other districts. What is most surprising, however, is not that e-hail produces fewer pickups in downtown areas than taxis, but that it does so with longer average wait and more vacant vehicles. Why does e-hail underperform in high-density areas, where the network effect is supposed to enhance its efficiency? To answer this question, we plot the average wait time in each local market against

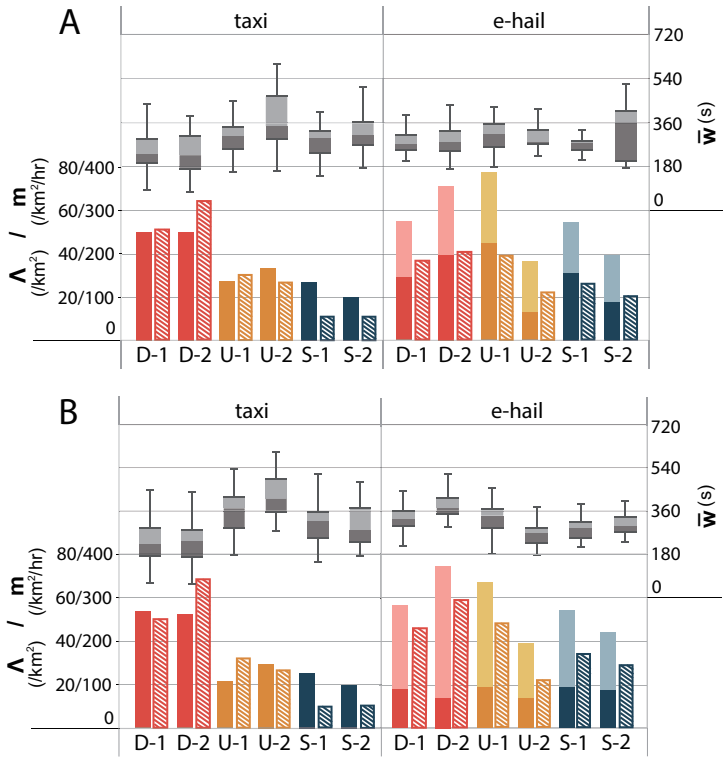

Figure 1: Aggregate service performance of taxis and e-hail by municipal districts. (**A**) Morning off-peak period (9:00-12:00). (**B**) Evening peak period (17:00-20:00). The districts are classified as downtown (D-1 and D-2), urban (U-1 and U-2), and suburban (S-1 and S-2); see Fig. S1. The solid bars represent average vacant vehicles per km^2 (Λ). For e-hail, the light- and dark-colored portions correspond to matched and unmatched vacant vehicles, respectively. The bars with diagonal lines represent hourly pickup rate (m). Average wait time ($\bar{w}$) is presented as box plots, where the boxes represent the 1st and 3rd quartiles and whiskers denote the highest/lowest datum within 1.5 IQR (i.e., the difference between the 1st and 3rd quartiles). For e-hail, average wait time is computed as the time elapsed from the order placement to the driver's arrival. For taxis, it is not directly observed but inferred based on calibrated models; see *Materials and Methods*).

two surrogates of the market scale: unmatched vacant vehicles and pickups.

Figs. 2(A) and (C) show that an increase in unmatched vacant vehicles reduces wait time for both taxis and e-hail. It confirms the network effect from the supply side, that is, bringing more drivers to the market benefits passengers. A closer look yields two observations. First, the taxi wait time is more sensitive to the change in supply. Second, e-hail lowers the likelihood of long waits (about 88% of e-hail markets have a 90th percentile wait time shorter than 10 minutes, compared to only 40% for taxis; see Fig. S2. On the demand side, Fig. 2(B) reveals

that average wait time for a taxi decreases as pickups increase, which indicates the demand-side network effect exists *for taxis* (i.e., the service gets better as more people use it). However, e-hail displays a puzzling picture: As the pickups grow, average wait time trends up mildly; see Fig. 2(D). This unexpected finding prompts us to hypothesize that *the network effect is undermined by a counter force in e-hail*.

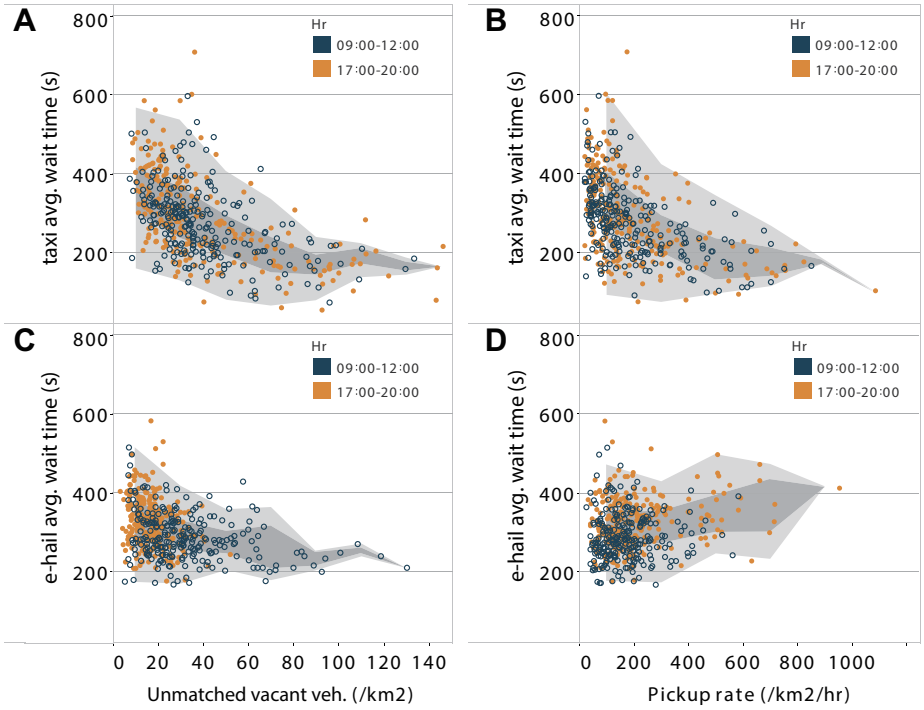

Figure 2: Relationship between average wait time, unmatched vacant vehicle density, and pickup rate. Each data point represents one local market at a given time period. The dark-gray areas are drawn with the 1st and 3rd quartiles of datum aggregated at an interval of 20/km^2 for free vacant vehicles and 200/km^2/hr for the pickup rate. The light-gray areas represent the same aggregated data within 1.5 IQR.

To test the above hypothesis, we analogize ride-hail to a process of trip production. The inputs to the production are waiting passengers and vacant vehicles, and the output is the trips (pickups). Using this analogy, the network effect can be measured by the production's *returns to scale*, that is, the rate of increase in output relative to the associated increase in the inputs. A positive (negative) network effect corresponds to increasing (decreasing) returns to scale; that

is, the production increases more (less) than the proportional change in all inputs. We model the trip production using the Cobb-Douglas function (*19*):

$$m = \beta(\Lambda\Pi)^{\alpha}, \tag{1}$$

where m is the hourly pickup rate (/km^2/hr); Λ is the density of vacant vehicles (/km^2); Π is the density of all waiting passengers (/km^2); β is the total factor productivity (TFP), determined by the production technology (i.e. the ride-hail's matching technology in this case); and α is the output elasticity to Λ and Π, which measures the sensitivity of production with respect to a change in inputs. The classic economic theory states that a production displays constant/increasing/decreasing returns to scale, when 2α is equal to/greater than/less than 1. We fit the linear equation $\log(m) = \log\beta + \alpha[\log(\Lambda) + \log(\Pi)]$ with estimates derived from the data for both taxi and e-hail. As shown in Fig. 3, e-hail's productivity is higher than that of taxis' by a factor of $\hat{\beta}^{ehail}/\hat{\beta}^{taxi} \simeq 15.89$, thanks to its significantly better matching technology. However, its trip production displays less than constant returns to scale ($2\alpha \simeq 0.9$), suggesting the overall network effect is negligible, if not negative. This finding is in sharp contrast to the taxis' production function, which shows strong increasing returns to scale ($2\alpha \simeq 1.6$).

The above empirical evidence indicates e-hail is not an unequivocal winner in the ride-hail industry. Equipped with better matching technology, e-hail mitigates passengers' exposure to long waits and significantly increases trip production in low-density areas. However, as e-hail attempts to scale up to serve more passengers, its efficiency is compromised by the loss of the network effect. In what follows, we show, paradoxically, the very technology that gives e-hail its advantages is also responsible for breaking the virtuous cycle of uberization.

Our theory centers on a passenger's ability to reach unmatched vacant vehicles around her; see Fig. 4. Assume the unmatched vacant vehicles distribute randomly in space with a density Λ_0. As the passenger gradually expands the search radius r, the number of unmatched vacant

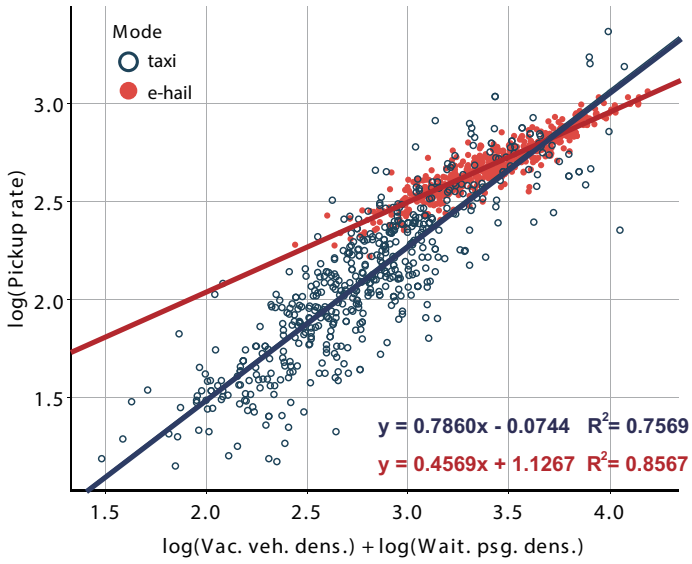

Figure 3: Empirical production functions for taxis and e-hail. Each data point represents one local market at a given time period. The fitted linear equations are reported at the lower-right corner, along with their goodness-of-fit R^2. The intercept measures the logarithm of TFP : $\log \hat{\beta}^{taxi} = -0.0744,\ \log \hat{\beta}^{ehail} = 1.1267$; the slope measures the output elasticity: $\hat{\alpha}^{taxi} = 0.7860,\ \hat{\alpha}^{ehail} = 0.4569$. Compared to taxis, e-hail enhances TFP by 1,489% ($\hat{\beta}^{ehail}/\hat{\beta}^{taxi} \simeq 15.89$), but lowers returns to scale by more than 40% ($\hat{\alpha}^{ehail}/\hat{\alpha}^{taxi} \simeq 0.58$), approaching constant returns to scale ($2\hat{\alpha}^{ehail} \simeq 0.9 < 1$). By contrast, taxis displays increasing returns to scale ($2\hat{\alpha}^{taxi} \simeq 1.6 > 1$).

vehicles increases at the rate of $2\pi r\Lambda_0$; see *Materials and Methods*. However, the passenger can only be matched with a fraction of these vehicles, denoted as $p(r)$, which is determined by a certain matching mechanism. Accordingly, we define $\lambda(r) = 2\pi r\Lambda_0 p(r)$ as the matching rate at r.

If the passenger hails a taxi off street, the fraction of matchable vacant vehicles $p(r)$ is limited by the maximum distance from which she can effectively communicate with a driver through eye contact or gesture. This distance is called the *hail radius* (denoted as d), which defines a circular *hail area* centered at the passenger's waiting location; see Figs. 4(A) and (C). Using simple geometry, we show $p(r)$ can be approximated by $(\sigma d)/(2\pi r)$, where σ is a correction factor that measures the attractiveness of the passenger's waiting location to nearby vacant taxis; see *Materials and Methods*. In the case of e-hail, $p(r)$ is no longer restricted by the hail radius, but rather by the density of passengers waiting to be matched ($\Pi_0 \leq \Pi$) and the

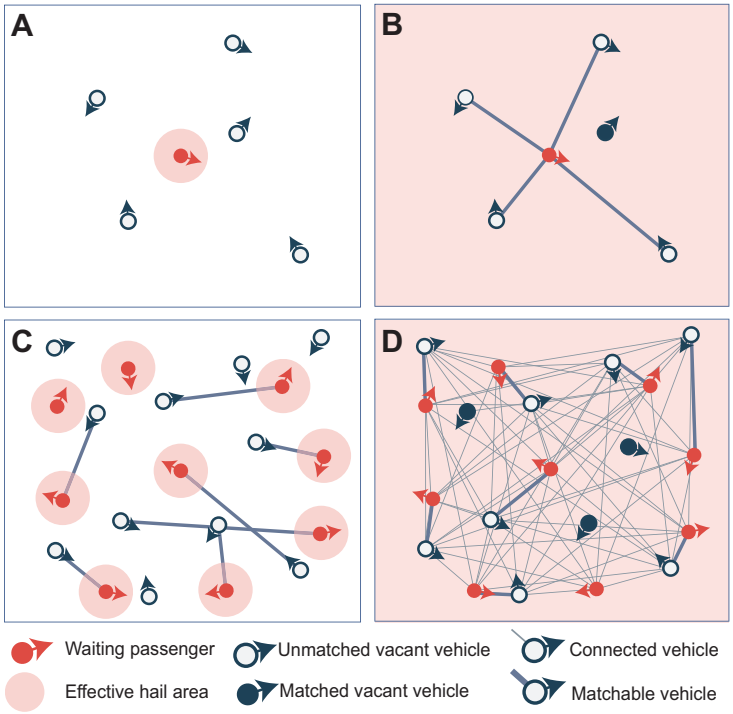

Figure 4: Illustration of the passenger-driver matching mechanism. (**A**) In a low-density area, none of the five vacant vehicles around the taxi passenger is matched with her. A matching occurs only if a taxi is projected to enter the passenger's hail area (the small red circle; see *Materials and Methods* for details). (**B**) In a low-density area, e-hail's matching technology expands the passenger's hail area dramatically. Hence, all four unmatched vacant vehicles are matchable for her. (**C**) Higher density improves taxi passengers' matching probability through the network effect. Only two out of nine passengers fail to find a matched vehicle. (**D**) Higher density forces the nine e-hail passengers to compete for the same eight unmatched vacant vehicles. The competition leaves one passenger without any matchable vacant vehicle.

efficiency of the matching algorithm (measured by a parameter k); see Figs. 4(B) and (D). We thus propose to approximate p with k/Π_0, assuming waiting passengers distribute randomly in the space and hence evenly share the unmatched vacant vehicles.

Suppose the passenger is picked up by the closest matchable vacant vehicle at r upon her arrival. Then, the passenger's wait time is $w = \delta r/v$, where v is the cruising speed of vacant vehicles and δ is a constant detour factor dependent on the topology of the road network (*20*). With mild assumptions, we show the cumulative distribution function (CDF) of passenger wait

time is

$$F(t) = 1 - \exp\left(-\int_0^t \lambda\left(\frac{vw}{\delta}\right)\frac{v}{\delta}\mathrm{d}w\right); \tag{2}$$

see *Materials and Methods*. Here, $\lambda_w = \lambda(vw/\delta)$ can be interpreted as the matching rate with respect to a wait time w. For taxi, $\lambda_w = \Lambda_0 d\sigma$, independent of w; for e-hail, λ_w increases with w linearly, that is $\lambda_w = (2\pi k\Lambda_0/\Pi_0)(vw/\delta)$. Because an e-hail passenger enjoys a greater matching rate as she waits longer, her exposure to a long wait is better mitigated than that of a taxi passenger. We attribute this advantage to e-hail's matching technology that effectively pushes the hail radius to infinity. This very advantage, however, is a mixed blessing. With an infinite hail radius, e-hail drags every waiting passenger into a competition for the same pool of unmatched vacant vehicles. The more passengers e-hail tries to serve, the stronger the competition and the smaller the average matching rate. Ironically, taxis are almost immune to such a competition, precisely because their hail radius is relatively small and does not create enough overlaps between passengers' hail areas. Consequently, although the network effect benefits taxis, it is neutralized in e-hail.

We proceed to validate the theory using the empirical findings presented earlier. Based on Eq. (2), the average wait time for taxis and e-hail can be derived respectively as

$$\bar{w}^{taxi} = \frac{\delta}{\sigma\Lambda_0 dv} = \frac{\delta}{\sigma\Lambda dv}; \quad \bar{w}^{ehail} = \frac{\delta}{2v}\sqrt{\frac{\Pi_0}{k\Lambda_0}} \simeq \frac{\delta}{2v}\sqrt{\frac{\Pi}{k\Lambda}}, \tag{3}$$

where d, σ, v, and k can be calibrated from data for each local market; see *Materials and Methods*. Hence, ceteris paribus, average wait time decreases as vacant vehicle density (Λ) increases in both services, yet the sensitivity is stronger in taxis than in e-hail ($\bar{w}^{taxi} \propto 1/\Lambda$ and $\bar{w}^{ehail} \propto 1/\sqrt{\Lambda}$). This result is consistent with the observations in Figs. 2(A) and (C). Furthermore, as per Little's formula (*21*), at the stationary state, the passenger arrival rate within a unit area, m, equals the average number of waiting passengers divided by average wait time, namely, $m = \Pi/\bar{w}$. Replacing Π in Eq. (3) with $m\bar{w}$ yields $\bar{w}^{taxi} \propto 1/m$ and $\bar{w}^{ehail} \propto m$.

Again, the theory prediction agrees with the empirical observations in Figs. 2(B) and (D).

Using the same stationary-state condition, the analytical Cobb-Douglas production function can be derived as follows:

$$m^{taxi} = \frac{\sigma d v}{\delta}\Pi\Lambda; \quad m^{ehail} = \frac{2v\sqrt{k}}{\delta}\sqrt{\Pi\Lambda}. \tag{4}$$

Eq. (4) implies taxi displays increasing returns to scale (both Λ and Π have an exponent $\alpha = 1$, so $2\alpha = 2$), whereas e-hail has constant returns to scale (both Λ and Π have an exponent $\alpha = 0.5$, so $2\alpha = 1$). This prediction matches well with the empirical results reported in Fig. 3, which show the returns to scale is 1.6 for taxis and 0.9 for e-hail. Eq. (4) also suggests e-hail's productivity is higher than that of taxis' by a factor of $\beta^{ehail}/\beta^{taxi} = 2\sqrt{k}/(\sigma d)$. We estimate $2\sqrt{k}/(\sigma d) \simeq 23.4$ with empirical results $d \simeq 36$ m, $\sigma \simeq 1.5$ and $k \simeq 0.4$; see Fig. S3. As a comparison, Fig. 3 shows the ratio between the productivity of e-hail and taxis is about 16, which is a reasonable agreement.

Discussion

To summarize, the analysis above reveals two opposing forces at work. On the one hand, aided by advanced matching technology, an e-hail passenger can access more vacant vehicles and is guaranteed to be matched with one at a greater rate as her wait time increases. In low-density areas, this advantage dramatically improves efficiency and lowers the likelihood of unpleasantly long waits. On the other hand, the technology is also trapped in an efficiency paradox. Connecting a large number of waiting passenger to the same pool of unmatched vacant vehicles induces competitions that undercuts the network effect and weakens the overall efficiency of the trip production. This negative impact is most prominent in high-density areas, where efficiency matters the most.

What lessons can we learn from this efficiency paradox? First, although uberization does

bring many positive changes to ride-hail, it has not made the industry much more efficient. Like taxis, hailing a ride with one's smart phone is unlikely to dominate public transportation. Second, the uberized transportation industry may not see a "winner-take-all." Simply scaling up may not help e-hail become more efficient, because the lack of a positive network effect leads to nearly constant returns to scale. Therefore, consumers can expect a variety of services provided by multiple firms with different value propositions.

We close by noting ride-hail is unlikely the only industry prone to the impact of the efficiency paradox. After all, the key insight here is simple and universal: Unless the service itself can be rendered more efficiently (e.g., by capacity sharing), quick match may only bring competition that undermines the overall efficiency. Uberization is continuing to reshape our everyday life, from grocery shopping (e.g., InstaCart), fund raising (e.g., GoFundMe) to education (e.g., VipKid). Therefore, it is important to understand which industries the paradox is likely to affect, the extent to which they are affected, and in what manner. We hope this work motivates others to examine this issue further, and that our theory finds applications beyond its domain.

Materials and Methods

Fraction of matchable vacant vehicle

The fraction of matchable vacant vehicles, denoted as $p(r)$, represents the main difference between taxis and e-hail in terms of matching. For taxis, a vacant vehicle is considered matchable if it satisfies: (i) it is cruising towards the passenger; i.e., its heading has an acute angle with its direction to the passenger ($\alpha < \pi/2$ in Fig. 5); (ii) it is traveling on the same side of the road as the passenger; i.e., its heading has an acute angle with the passenger's travel direction ($\beta < \pi/2$ in Fig. 5); and (iii) either it is in the passenger's effective hail area (Fig. 5(D)), or it will eventually enter the passenger's effective hail area if it continues on its current path

(Fig. 5(E)).

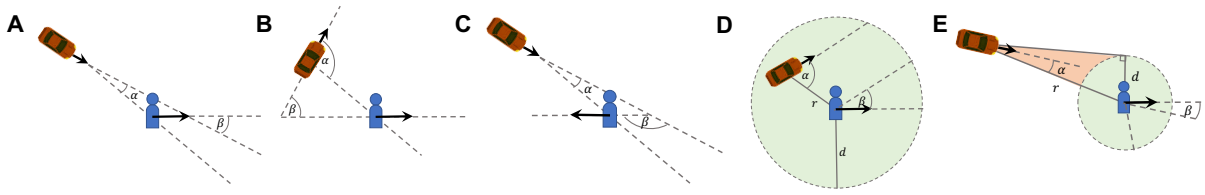

Figure 5: Illustration of matchable vacant taxi. (**A**) A vehicle that satisfies conditions (i) and (ii). (**B**) A vehicle violates condition (i). (**C**) A vehicle violates condition (ii). (**D**) A matchable vehicle inside the effective hail area. (**E**) A matchable vehicle outside the effective hail area.

Accordingly, the fraction of matchable vehicles $p(r)$ given EHD d can be derived with respect to r using simple geometry (*22*).

$$p(r) = \begin{cases} \frac{1}{4} & r \leq d \\ \frac{1}{2\pi} \arcsin(d/r) & r > d \end{cases} \tag{5}$$

Consider the rare possibility of observing a matchable vehicle inside the effective hail area upon the passenger's arrival, we only use the second case of Eq. (5) in model calibration. Further, because the pickup vehicle is often far away from the passenger as he arrives, we apply the approximation $\arcsin(d/r) \approx d/r$, which finally yields $p(r) = d/(2\pi r)$.

Distribution of passenger wait time

The passenger wait time is derived from a physical model of passenger–driver matching process. Consider the moment when a passenger arrives. We define a *counting process* $\tilde{N}(r)$ as the number of unmatched vacant vehicles within a distance r from the passenger. Assume (i) all unmatched vacant vehicles are cruising at the same speed v, (ii) unmatched vacant vehicles are uniformly distributed with spatial density Λ, and (iii) the passenger keeps waiting at the same location until finally being picked up. Then, we prove that $\tilde{N}(r)$ is an *Inhomogeneous Poisson Process* with intensity function $\eta(r) = 2\pi\Lambda_0 r$ (*22*).

For each unmatched vacant vehicle at distance r from the passenger, $p(r)$ determines the

probability that the vehicle is matchable for the passenger. Because the matchability of one vehicle is independent of that of others, $\tilde{N}(r)$ can be split into two independent sub-processes, corresponding to counting matchable and unmatchable vehicles. Therefore, the number of matchable vehicles, denoted as $\tilde{N}_1(r)$, is also an Inhomogeneous Poisson Process with intensity function $\eta_1(r) = 2\pi\Lambda_0 r p(r)$.

Suppose the passenger is picked up by the closest matchable vehicle, and denote $\tilde{D}$ as its distance to the passenger at the time when she enters the market. Then, the passenger wait time $\tilde{w} = \delta\tilde{D}/v$, where δ is a constant detour factor that corrects the vehicle's travel distance prior to the pickup. Accordingly,

$$P(\tilde{w} \leq t) = 1 - P(\tilde{N}_1(vt/\delta) = 0) = 1 - \exp\left[-\int_0^t \frac{2\pi\Lambda_0 v^2 w}{\delta^2} p(vw/\delta)\mathrm{d}w\right]. \tag{6}$$

Plugging in $p(r) = (\sigma d)/(2\pi r)$, $\Lambda = \Lambda_0$ for taxis and $p(r) = k/\Pi_0$, $\Lambda/\Pi \simeq \Lambda_0/\Pi_0$ for e-hail, we finally derive the CDF of passenger wait time in each service as

$$F^{taxi}(t) = 1 - \exp\left(-\frac{\sigma\Lambda d v}{\delta}t\right); \tag{7}$$

$$F^{ehail}(t) = 1 - \exp\left(-\frac{\pi k\Lambda v^2 t^2}{\delta^2\Pi}\right), \tag{8}$$

which yield the average wait time in Eq. (3).

Local ride-hail market

To calibrate the model, we need properly specify a local market. In this study, a local market for a given ride-hail service is defined by the combination of a core area and a time period. We select 277 core areas, each corresponding to one or several traffic analysis zones (TAZ) defined by the city's urban planning agency. Two time periods—a morning off-peak period (10 AM–12 PM) and an evening peak period (5 PM–8 PM) are selected. Thus, in total we create 277×2 local markets for each service. It should be noted that the demand and supply in each local

market are not necessarily confined by the physical boundary of the core area. Instead, they are defined differently for taxis and e-hail, according to the operational characteristics of these services.

For taxis, we consider the demand as all pickups in the core area, and for each pickup, we define a "supply area" centered at the pickup location. The size of the supply area is selected to cover matchable vehicles within a reasonable distance, thus it often goes beyond the core area. For simplicity, in this study we set the supply area to be a square centered at the pickup location with an area of about 1 km^2. The reader is referred to (*22*) for more details about the supply area.

To specify the supply area for e-hail, we first find the centroid of all pickup locations recorded inside the core area, and then, centering at that point, draw a circle with a radius equal to 90th percentile of all pickup distances (the green circle in Fig. 6). Defining the demand is more complicated, because a passenger waiting in the core area may compete with those both inside and outside the supply area. For example, the passenger outside the supply area is competing with passengers in the study area as he/she may be closer to a vacant vehicle in the supply area; see Fig. 6(B). Therefore, we need to consider waiting passengers in an even larger area, called the "competing area" (the orange circle in Fig. 6). The competing area is defined as a circle that is concentric with the supply area but doubles its radius. Accordingly, waiting passengers in the competing area who compete for vacant vehicles in the supply area contribute to the demand in this local market, which will be further specified in the following section.

Aggregate measures

Given the definition of demand and supply, three aggregate measures are estimated in each local market, i.e., vacant vehicle density Λ, waiting passenger density Π and pickup rate m. For taxis, the vacant vehicle density is estimated in the same way as described in *(22)*, which is equivalent

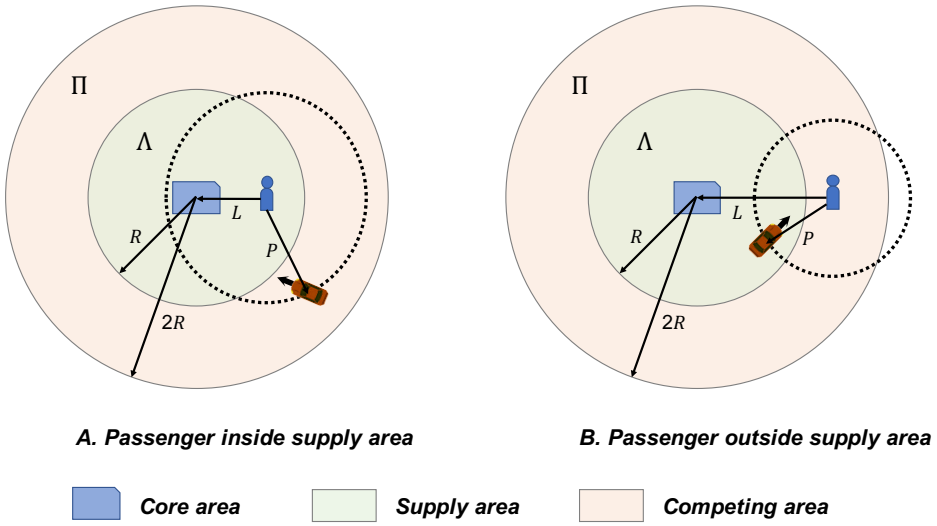

Figure 6: Illustration of the local e-hail market. (**A**) Potential competing passenger inside the supply area. (**B**) Potential competing passenger outside the supply area.

to the unmatched vacant vehicle density, i.e., $\Lambda = \Lambda_0$. Waiting passenger density and pickup rate are given by

$$\Pi = \frac{1}{\mu HC} \sum_{i=1}^{N} t^i; \quad m = \frac{N}{\mu HC}, \tag{9}$$

where H is the length of analysis time period, N is the number of pickups observed in the core area within H, μ is the sample rate (see [S1.2] in *Supplementary Materials* for more details), t^i is the passenger wait time of ith pickup, and C is the core area. Since the exact passenger wait time is not available from the taxi data, multiple random draws are first taken based on the calibrated model. For each draw, we compute Π from Eq. (9), then the sample average is used as the final estimate.

For e-hail, the unmatched vacant vehicle density Λ_0 is directly obtained from data. Estimating matched vacant vehicle density Λ_1 and waiting passenger density, however, is more complicated and has to be addressed in the competing area. For each pickup observed in the competing area, we need to determine (i) the probability that the pickup is associated with the local market, denoted as p, and (ii) when $p > 0$, how much it contributes to the matched vacant

vehicle density, which is quantified by P_c, a fraction of its pickup distance. Since the pickup trajectories are not observed, we propose different approximations of p and P_c based on the potential competing passenger's pickup location. See [S1.1] in *Supplementary Materials* for details.

Given the specification of p and P_c for each pickup, the waiting passenger density and matched vacant vehicle density are finally estimated as

$$\Pi = \frac{1}{\mu H \pi R^2} \sum_{i=1}^{N^c} t^i p^i, \quad \Lambda_1 = \frac{1}{\mu H \pi R^2} \sum_{i=1}^{N^c} t^i \frac{P_c^i}{p^i}, \tag{10}$$

where N^c is the number of pickups observed in the competing area.

Finally, two different pickup rates are computed for e-hail. In Fig. 1 and 2, pickup rates are computed in core areas so that the magnitude of the rates is comparable to that for taxis, i.e. they are measured for exactly the same area. In Fig. 3, the pickup rates for e-hail are computed with respect to each local market, i.e.,

$$m^c = \frac{1}{\mu H \pi R^2} \sum_{i=1}^{N^c} p^i. \tag{11}$$

This is necessary because here we aim to examine the production function of local markets. To that end, the output of the local market must include all pickups associated with it (not just those in its core area), as clarified in the above explanation.

Calibration of taxi model

The taxi model is calibrated using taxi GPS trajectory data. See [S1.2] in *Supplementary Materials* for more details. Because the exact passenger wait time of each pickup is not directly observed from the available data of taxis, we develop a method to extract the maximum possible wait time. We prove that, under mild conditions, the maximum possible wait time follows the same distribution of passenger wait time given the EHD value. Using this important property, d and σ can be estimated using an iterative algorithm (*22*).

A critical step in the calibration is to construct the empirical mapping from each possible wait time to the maximum possible EHD. In short, we determine the upper bound of EHD by the distance from the pickup location to the pickup vehicle during its cruising phase (when it must not be engaged with the passenger) and to the closest other matchable vehicles, which requires trajectories of all vacant vehicles. However, in practice we do not always have full access to the data or sometimes there is a considerable amount of errors in the data. Here we show the passenger maximum wait time can still be properly estimated when trajectory data are incomplete.

Assume that: (i) observed and unobserved vacant vehicles are randomly and independently distributed in the supply area with density Λ^o and Λ^u, respectively; (ii) all other parameters, i.e. v, d and σ, are the same among observed and unobserved vacant vehicles; and (iii) the ratio between unobserved and observed vacant vehicles is known, denoted by μ. Following the same derivation as in (*22*), we can prove that the number of observed and unobserved matchable vehicles within a distance r from the passenger, denoted by $\tilde{N}_1^o$ and $\tilde{N}_1^u$, are Homogeneous Poisson Processes with intensity functions $\eta_1^o = \Lambda^o d$ and $\eta_1^u = \Lambda^u d$, respectively, Thanks to the independence, $\tilde{N}_1^o$ and $\tilde{N}_1^u$ merge into a Homogeneous Poisson Process $\tilde{N}_1$ with intensity $\eta_1 = (\Lambda^o + \Lambda^u)d = (1+\mu)\Lambda^o d$. Accordingly, the average wait time is

$$E[\tilde{w}^s] = \frac{\delta}{\sigma v \Lambda d} = \frac{\delta}{\sigma v (1+\mu)\Lambda^o d}. \tag{12}$$

The main difficulty lies in building the empirical mapping g, as we no longer observe the exact distance from the closest other matchable taxi to the pickup location. Given a possible wait time w, we denote d_M^o and d_M^u as the distance from the closest observed and unobserved matchable taxi to the passenger, respectively. In essence, we need the maximum possible EHD

as $d_M = \min\{d_M^o, d_M^u\}$. Due to the missing data, we approximate d_M by taking its expectation

$$\begin{aligned} E[d_M] &= d_M^o P(d_M^o < d_M^u) + E[d_M^u | d_M^o \geq d_M^u] \\ &= \frac{1 - e^{-\sigma \Lambda^u d d_M^o}}{\sigma \Lambda^u d} = \frac{1 - e^{-\sigma \mu \Lambda^o d d_M^o}}{\sigma \mu \Lambda^o d}. \end{aligned} \tag{13}$$

When d_M^o is very small, it is easily verified that $\sigma \mu \Lambda^o d d_M^o \to 0^+$. Hence, the Taylor expansion at 0^+ gives

$$E[d_M] = \frac{1 - [1 - \sigma \mu \Lambda^o d d_M^o + o(\sigma \mu \Lambda^o d d_M^o)]}{\sigma \mu \Lambda^o d} \approx d_M^o. \tag{14}$$

As d_M^o increases, $E[d_M]$ gradually deviates from d_M^o and approaches $E[d_M^u] = 1/(\sigma \Lambda^u d)$. Therefore, $E[d_M]$ is well bounded between d_M^o and $1/(\sigma \Lambda^o d)$. Note that the gap between the lower and upper bounds grows as d, σ or μ increases, because there would be a larger probability mass for small realizations of d_M^u. Examples of observed and corresponding expected maximum EHD are illustrated in Fig. 7).

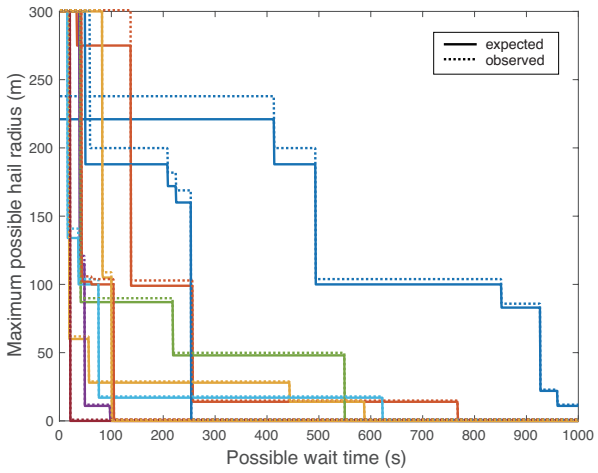

Figure 7: Sample empirical mappings with and without consideration of missing data. The other parameters are $\Lambda = 46.93$ /km^2, $v = 2.5$ m/s, $\mu = 0.8315$, $d = 15$ m and $\sigma = 1.0$.

Since computing $E[d_M]$ requires d and σ, we develop an iterative calibration algorithm with two loops. The inner-loop performs the calibration procedure introduced in *(22)*, while $\hat{d}$ and

$\hat{\sigma}$, as well as the empirical mapping, are updated in the outer-loop. The initial estimates are generated without consideration of the missing data. $\hat{d}$ and $\hat{\sigma}$ are then updated by

$$\hat{d}_{out}^{k} = \hat{d}_{out}^{k-1} + \iota(\hat{d}_{in}^{k-1} - \hat{d}_{out}^{k-1}), \tag{15}$$

$$\hat{\sigma}_{out}^{k} = \hat{\sigma}_{out}^{k-1} + \iota(\hat{\sigma}_{in}^{k-1} - \hat{\sigma}_{out}^{k-1}), \tag{16}$$

where $\hat{(\cdot)}_{in}, \hat{(\cdot)}_{out}$ are estimates in the inner- and outer-loop, respectively, and ι is a constant moving step (set to be 0.5 in this study).

Calibration of e-hail model

The e-hail model is calibrated using a random sample of trip records and cruising time of uncommitted vacant vehicles aggregated in each period and spatial units. See [S1.2] in *Supplementary Materials* for more details. Given the estimates of Λ and Π as per Eq. (10), the two parameters remained to be calibrated are the cruising speed v and the matching parameter k. For simplicity, v is estimated by the average pickup velocity of all pickups observed in the core area. From Eq. (8), we derive the probability density function of passenger wait time as

$$f^{ehail}(t) = \frac{2\pi k \Lambda v^2 t}{\delta^2 \Pi} \exp\left(-\frac{\pi k \Lambda v^2 t^2}{\delta^2 \Pi}\right). \tag{17}$$

Accordingly, the log-likelihood function of k is constructed as

$$\begin{aligned}\mathcal{L}(k) &= \log \prod_{i=1}^{N} f^{ehail}(t^i) \\ &= \sum_{i=1}^{N} \log\left(\frac{2\pi \hat{\Lambda} \hat{v}^2 t^i}{\delta^2 \hat{\Pi}}\right) + N \log k - \frac{\pi k \hat{\Lambda} \hat{v}^2}{\delta^2 \hat{\Pi}} \sum_{i=1}^{N} (t^i)^2. \end{aligned} \tag{18}$$

where t^i is the observed passenger wait time of the ith pickup.

Maximizing Eq. (18) thus yields the maximum log-likelihood estimator for k as

$$\hat{k} = \frac{N \delta^2 \hat{\Pi}}{\pi \hat{\Lambda} \hat{v}^2 \sum_{i=1}^{N} (t^i)^2}. \tag{19}$$

Supplementary Materials

References

1. R. H. Coase, The nature of the firm. *economica*. **4**, 386 (1937).

2. G. F. Davis, What might replace the modern corporation: Uberization and the web page enterprise. *Seattle UL Rev.*. **39**, 501 (2015).

3. N. Daidj, *Advanced Methodologies and Technologies in Digital Marketing and Entrepreneurship* (IGI Global, 2018), pp. 116–128.

4. G. Zervas, D. Proserpio, J. W. Byers, The rise of the sharing economy: Estimating the impact of airbnb on the hotel industry. *Journal of marketing research*. **54**, 687 (2017).

5. F. Caldieraro, J. Z. Zhang, M. Cunha Jr, J. D. Shulman, Strategic information transmission in peer-to-peer lending markets. *Journal of Marketing*. **82**, 42 (2018).

6. S. Yao, C. F. Mela, Online auction demand. *Marketing Science*. **27**, 861 (2008).

7. M. Rysman, The economics of two-sided markets. *Journal of economic perspectives*. **23**, 125 (2009).

8. C. Tucker, J. Zhang, Growing two-sided networks by advertising the user base: A field experiment. *Marketing Science*. **29**, 805 (2010).

9. M. A. Cusumano, The sharing economy meets reality. *Communications of the ACM*. **61**, 26 (2017).

10. Z. Guzman, Why lyft's ipo may be more attractive than uber's. *Yahoo Finance* (2019).

11. G. W. Douglas, Price regulation and optimal service standards: The taxicab industry. *Journal of Transport Economics and Policy*. pp. 116–127 (1972).

12. R. Arnott, Taxi travel should be subsidized. *Journal of Urban Economics*. **40**, 316 (1996).

13. H. Yang, S. Wong, A network model of urban taxi services. *Transportation Research Part B: Methodological*. **32**, 235 (1998).

14. L. Zha, Y. Yin, H. Yang, Economic analysis of ride-sourcing markets. *Transportation Research Part C: Emerging Technologies*. **71**, 249 (2016).

15. J. Castillo, D. T. Knoepfle, E. G. Weyl, Surge pricing solves the wild goose chase (2018). Available at SSRN: `https://ssrn.com/abstract=2890666`.

16. J. Cramer, A. B. Krueger, Disruptive change in the taxi business: The case of uber. *American Economic Review*. **106**, 177 (2016).

17. E. M. Azevedo, E. G. Weyl, Matching markets in the digital age. *Science*. **352**, 1056 (2016).

18. Y. M. Nie, How can the taxi industry survive the tide of ridesourcing? evidence from shenzhen, china. *Transportation Research Part C: Emerging Technologies*. **79**, 242 (2017).

19. C. W. Cobb, P. H. Douglas, A theory of production. *American Economic Review*. **18**, 139 (1928).

20. H. Yang, J. Ke, J. Ye, A universal distribution law of network detour ratios. *Transportation Research Part C: Emerging Technologies*. **96**, 22 (2018).

21. J. D. Little, A proof for the queuing formula: L= λ w. *Operations research*. **9**, 383 (1961).

22. H. Chen, K. Zhang, X. Liu, Y. M. Nie, A physical model of street ride-hail (2018). Available at SSRN: `https://ssrn.com/abstract=3318557`.

Acknowledgments

This work is partially supported by the National Science Foundation under the award number PFI:BIC 1534138 and by National Science Foundation of China (NSFC) under the award number 71671147. L.X., J.G., X.L. collected the data; K.Z., H.C., S.Y., Y.N. analyzed the data; H.C., K.Z., Y.N. developed and calibrated the model. Y.N. supervised the project. All authors contributed to writing the manuscript. Correspondence and requests for materials should be addressed to Y.N. (y-nie@northwestern.edu). We wish to thank Professors Kimberly Gray, Luis Amaral, Julio Ottino, Dashun Wang and Ian Savage at Northwestern University, Professor Emeritus Ken Small at University of California Irvine, and Professor Kathleen Vohs at University of Minnesota for their helpful comments on earlier versions of the paper.

Supplementary Materials for An efficiency paradox of uberization

Kenan Zhang, Hongyu Chen*, Song Yao, Linli Xu, Jiaoju Ge,
Xiaobo Liu, Yu (Marco) Nie
Correspondence to: y-nie@northwestern.edu.

This PDF file includes:

1. Supplementary Text
2. Fig. S1. Distribution of selected core areas in Shenzhen.
3. Fig. S2. Histogram of 90-percentile passenger wait time in each local market.
4. Fig. S3. Main results of model calibration.
5. Fig. S4. Cases of potential competing passenger inside the supply area of an e-hail local market.
6. Fig. S5. Cases of potential competing passenger outside the supply area of an e-hail local market.
7. Fig. S6. Simple validation of estimated average passenger wait time.

*These authors contributed equally to the work .

S1 Supplementary Text

S1.1 Scenarios of potential competing passengers in e-hail local markets

Consider a pickup in the competing area (orange circle in Figs. S4 and S5). Let P be the pickup distance, L be the distance from the pickup location to the center of the market, and R be the radius of supply area. We specify the probability of the pickup belonged to the local market (p) and the pickup distance contributing to the matched vacant vehicle density (P_c) for the following two cases, each of which has three subcases.

1. The pickup is located inside the supply area, i.e., $L \leq R$.

   (a) $P \leq R - L$ (Fig. S4(A)): In this subcase, the pickup vehicle must start inside the supply area. Hence, the passenger associated with the pickup is definitely part of the demand in the market and the entire pickup distance should be counted in the matched vacant vehicle density, i.e., $p = 1$ and $P_c = P$.

   (b) $P > R+L$ (Fig. S4(B)): In this subcase, the pickup vehicle starts outside the supply area. Hence, the passenger did not compete for the supply inside the supply area of the market. Then pickup event has no contribution to either demand or supply. $p = 0$ and $P_c = 0$.

   (c) $R - L < P \leq R + L$ (Fig. S4(C)): In this subcase, the pickup may or may not start inside the supply area. The probability that it starts inside can be computed as $p = \theta_1/\pi$, where θ_1 can be solved by the law of cosine (i.e., $R^2 = L^2 + P^2 - 2LP\cos\theta_1$). Accordingly, the contribution of the pickup distance to the matched vacant vehicle density is $P_c = P\theta_1/\pi$.

2. The pickup is located outside the supply area, i.e., $L \leq R$.

(a) $P \leq L - R$ (Fig. S5(A)): In this subcase, the pickup vehicle must start outside the supply area. As per the argument in 1(b), $p = 0$ and $P_c = 0$.

(b) $P > L + R$ (Fig. S5(B)): $p = 0$ and $P_c = 0$ for the same reason as in 1(b).

(c) $L - R < P \leq L + R$ (Fig. S5(C)): Similar to 1(c), the probability that the pickup vehicle starts inside the supply area is θ_1/π. However, only a fraction of the pickup distance is covered by the supply area. To be consistent with the estimate of matched vacant vehicle density, we count a cropped distance $P' = P - L\cos\theta + \sqrt{R^2 - (L\sin\theta)^2}$, and approximate the average of P' by

$$\begin{aligned} \bar{P'} &= \frac{1}{\pi}\int_0^{\theta_1} \left(P - L\cos\theta + \sqrt{R^2 - (L\sin\theta)^2}\right) \mathrm{d}\theta \\ &\approx \frac{\theta_1}{\pi}P - \frac{\sin\theta_1}{\pi}L + \frac{1}{\pi}\sqrt{\theta_1^2\left(R^2 - \frac{L^2}{2}\right) + \frac{\theta_1 \sin 2\theta_1}{4}L^2}. \end{aligned} \tag{S1}$$

Hence, the contribution of the pickup distance to the matched vacant vehicle density is given by $P_c = \bar{P'}\theta_1/\pi$.

S1.2 Data description

The data of both taxis and e-hail services are collected in Shenzhen, China for a week in 2016. The taxi data consist of GPS trajectories of all registered taxis in the city over the study period with an average inter-record interval of 20 seconds. Each GPS record contains information including taxi license ID, time stamp, coordinates, instantaneous speed and heading, and passenger occupancy status (0/1 variable). Using the procedure described in *(18)*, trajectories are first segmented according to flips in the occupancy status, generating 250 to 300 thousand daily occupied trips. The e-hail data consist of a random sample of trip records and cruising time of uncommitted vacant vehicles aggregated in each time period and spatial unit. The trip records are randomly selected with a sample rate of 6%, producing about 45 thousand trips per day.

Each trip record includes coordinates of the trip origin and destination, order placement time, driver arrival time, trip starting/ending time, pickup distance, etc.

S1.3 Main calibration results

Fig. S3 reports main calibration results. EHD estimates narrowly range between 30-45 meters, with a median of 36 meters across all local markets. σ estimates range between 1 and 3, with a median of about 1.5. These findings well match the physical meaning of the two parameters in the taxi model. As for e-hail, estimated values for the matching efficiency parameter k vary significant across the markets, from as low as close to zero to as high as more than 3. However, no correlation with the waiting passenger density is noticed. The median of k is about 0.415. Fig. S6 compares the estimated and observed average passenger wait times for the purpose of validation. It shows that e-hail models tend to have better goodness-of-fit, likely because the data used in their calibration are of higher quality (they are actual observations of passenger wait time). As expected, a lower sample rate leads to worse goodness-of-fit; see Fig. S6(B).

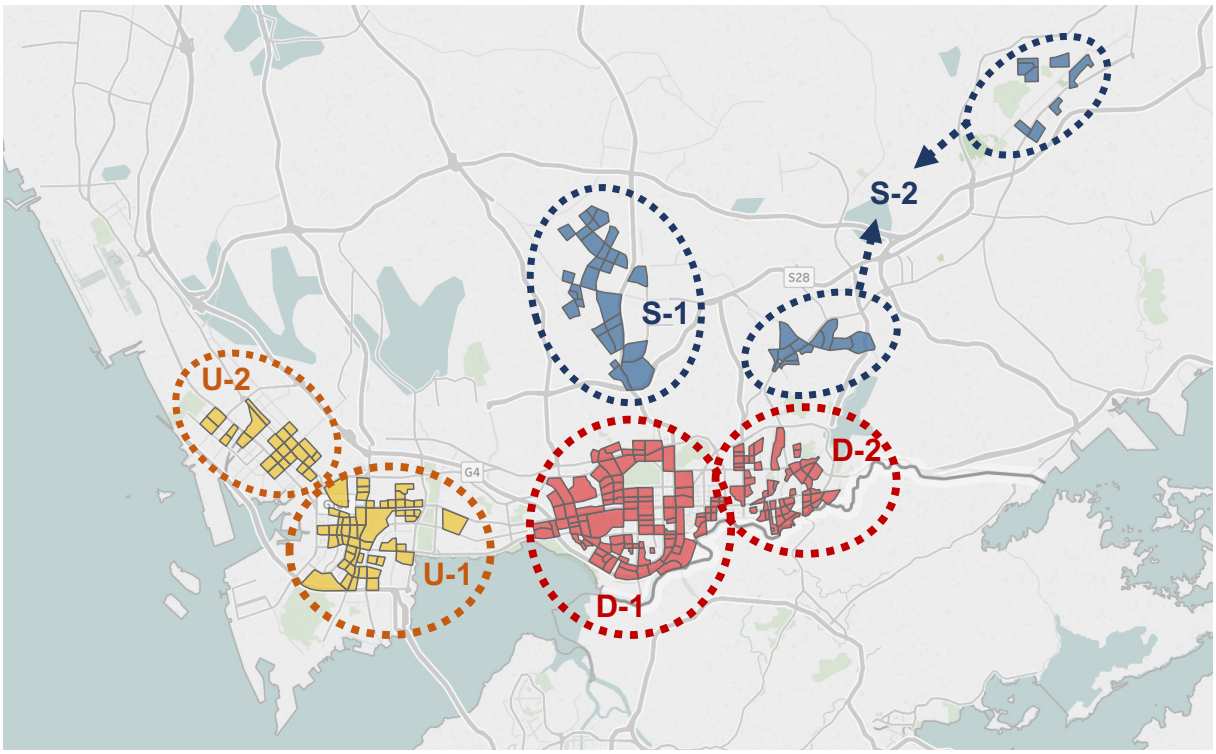

Figure S1: Distribution of selected core areas in Shenzhen. The 277 core areas are distributed in the six municipal districts in Shenzhen.

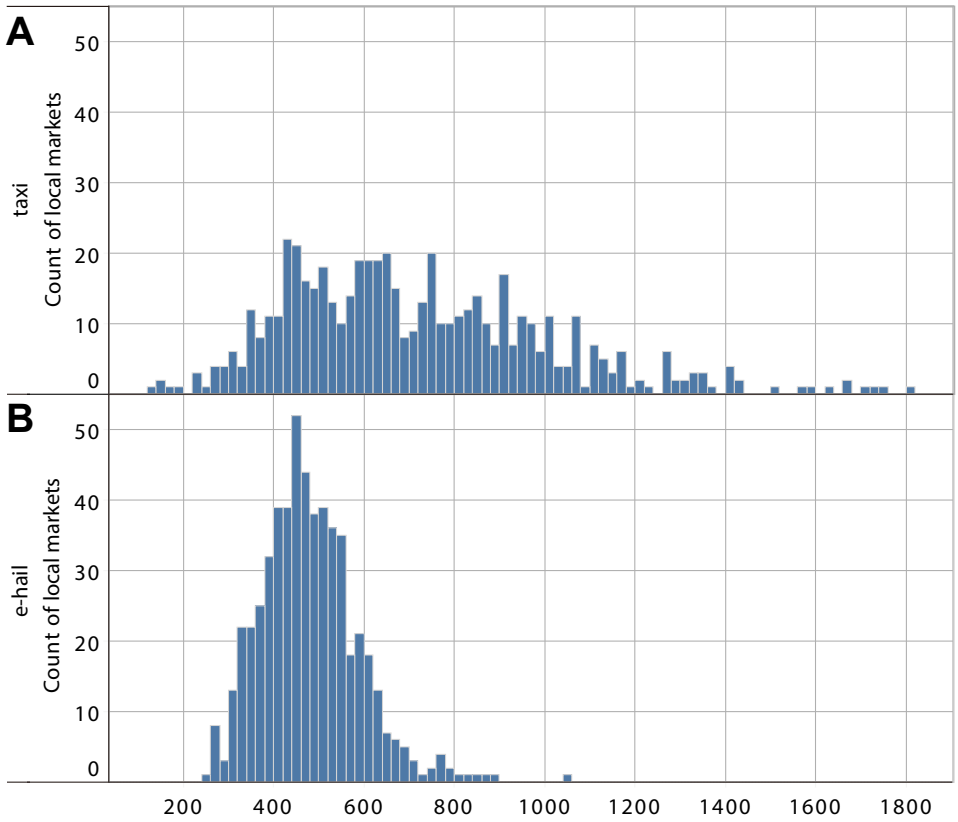

Figure S2: Histogram of 90-percentile passenger wait time in each local market. (**A**) Taxi; and (**B**) e-hail.

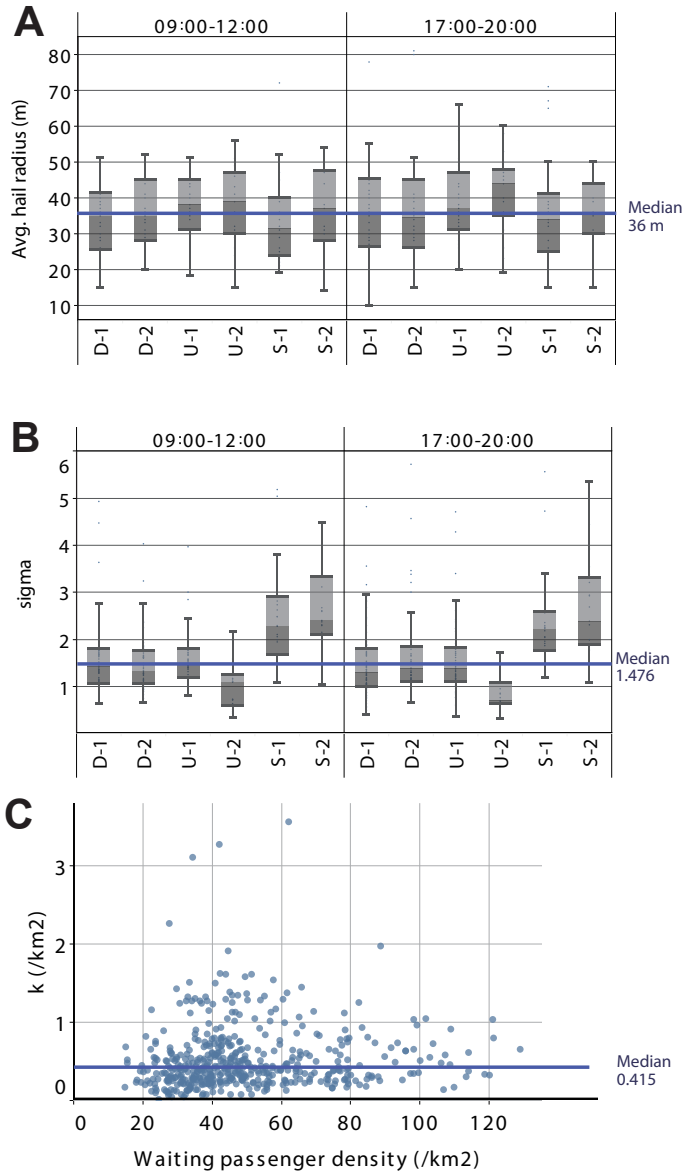

Figure S3: Main results of model calibration. (**A**) Boxplots of EHD estimates by municipal district and time period. (**B**) Boxplots of σ estimates by municipal district and time period. (**C**) Estimates of k against waiting passenger density. The median estimate values over all local markets are also illustrated in each subplot.

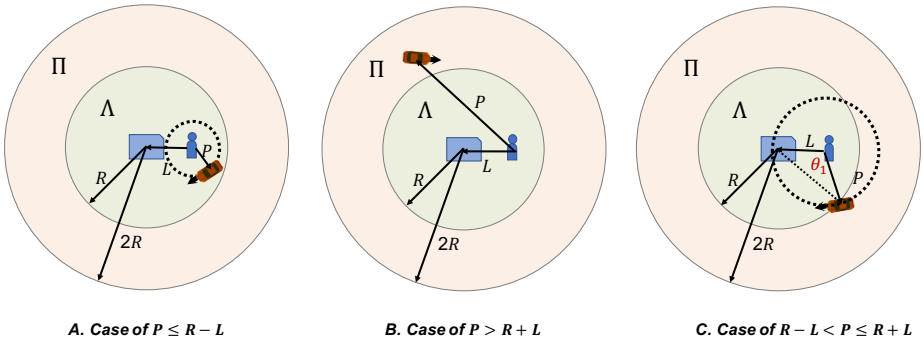

Figure S4: Cases for potential competing passenger inside the supply area.

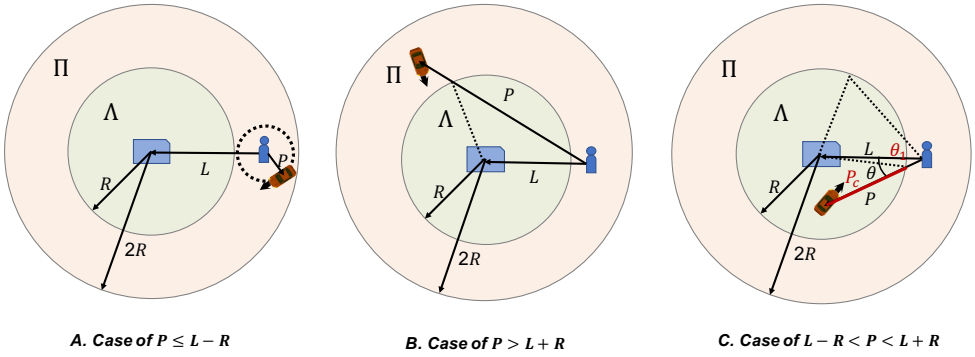

Figure S5: Cases for potential competing passenger outside the supply area.

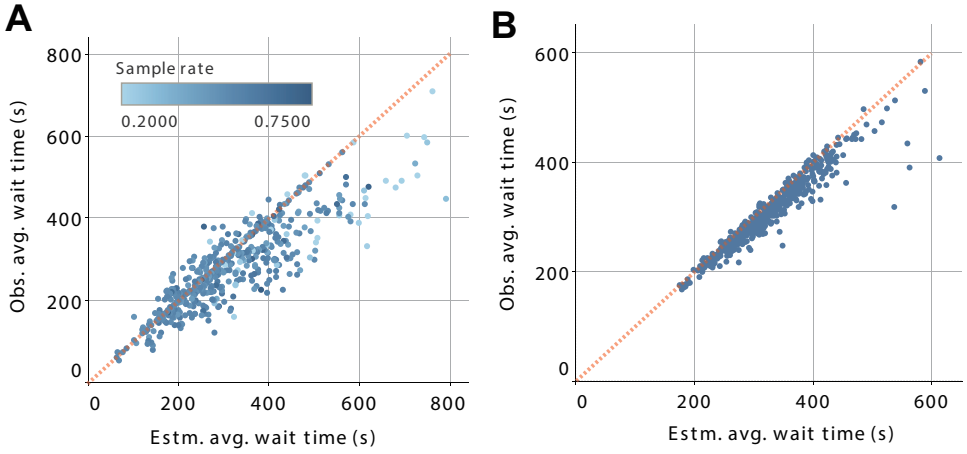

Figure S6: Simple validation of estimated average passenger wait time. (**A**) Taxi; and (**B**) e-hail. Points on the diagnoal dash line mean the model make correct predictions. The color of each point represents the sample rate.